Kamal *et al.*
Journal of Engineering and Applied Science (2023) 70:13
https://doi.org/10.1186/s44147-023-00181-0

Journal of Engineering and Applied Science

RESEARCH Open Access

Performance characteristic of a PV module as influenced by dust accumulation: theory versus experiment

Reham Kamal*, Mazen Abdel-Salam and Mohamed Nayel

*Correspondence:
reham.ramadan@aun.edu.eg

Department of Electrical Engineering, Faculty of Engineering, Assiut University, Assiut, Egypt

Abstract

This paper is aimed at assessing by theory and experiment the current–voltage and power-voltage characteristics of a PV module as influenced by dust accumulation. A method is proposed in a computer code to follow-up an incident solar radiation through the module layers considering the reflection and transmission of radiation at the interfaces between the layers to evaluate how the incident radiation is attenuated before reaching the module. Also, absorption of radiation in the dust layer and the glass cover is considered. The evaluation of the reflectance and transmittance calls for analysis of the accumulated dust to identify its constituents using X-ray fluorescence apparatus. The refractive and absorption indices are assessed for dust constituents as well as the corresponding effective values for the sample as a whole. The current–voltage characteristic of the dusty module is calculated using Simulink with consideration of module parameters after being corrected according to the incident radiation received by the solar cell and the ambient temperature where the module is installed. The calculated current–voltage and power-voltage characteristics of the dusty module agreed reasonably with the measured ones for a 175-W module as the incident radiation decreased to 68% due to dust accumulation with a subsequent decrease of the maximum output power of dusty module by 31% when compared with the clean one. The percentage decrease of short-circuit current recorded 31% due to dust deposition against 2% for the increase of open-circuit voltage at ambient temperature of 44 °C and incident solar radiation of 1027 W/m^2. This conforms to previous findings in the literature.

Keywords: PV module, Dust accumulation, Solar radiation, Reflection, Transmission, Absorption, Reflectance, Transmittance, Maximum output power

Introduction

Nowadays, renewable energy has a great importance, especially with the depletion of fossil fuel. Therefore, the world is looking for sustainable efficient renewable sources. One of these sources is harnessing solar energy in PV systems. To improve the utilization efficiency of these systems, maximum power point tracking (MPPT) techniques were developed. The performance of PV systems is influenced by many factors that affect their efficiency such as shading, temperature, and dust accumulation on solar modules,

especially in desert regions. Dust accumulation on the surface of the PV cell is one of the most important and common causes of efficiency loss as well as modules degradation.

The demand for electricity in Egypt shows a significant rise due to the increase of population and expansion in energy infrastructure and industrial projects. It reached 27.6 gigawatt (GW) in 2019 and is expected to reach 67 GW by 2030 [1]. This motivated the government to build large combined-cycle power plants and adopt renewable energy projects to harness wind and solar energy, in order to increase the installed capacity, fulfill demand, and ensure economic growth. Renewable energy targets of the Egyptian government in 2035 are to increase the installed capacity by 42% including 14% by wind generation, 22% by PV generation, 4% by concentrated solar power, and 2% by hydro [2]. One of the huge projects that the government has set to achieve its renewable energy targets through commissioning the Benban Solar Park with 1465 megawatt (MW) installed capacity. Benban is a power complex of 41 solar power plants, which was connected to the electricity grid in September 2019. The Benban project is located in Aswan governorate in Upper Egypt in desert area, which suffer from high temperature and dusty atmosphere. In this extreme environment, the accumulation of dust and high ambient temperature characterizing this environment reflect themselves on the performance of Benban plant.

The accumulation of dust has a negative impact on the PV power outputs, and assessment of such dust accumulation may be an avenue to predict appropriate time to clean the photovoltaic modules for enhancing the power output. A research paper studied the effect of dust deposits on the PV modules' surface [3] and found reduction of output efficiency by 26% with increase of deposition density to 22 g m^{-2}. An experimental study has been conducted [4] to assess dust deposition density and transmission coefficient of solar radiation through a glass sample oriented in eight geographical directions. In each direction, the glass sample was oriented along seven directions spaced equally over the range from 0 to 90°. The dust deposition density was found to vary from 4 g m^{-2} for northwest orientation of the glass samples at angle 90° up to 10.3 g m^{-2} for north orientation at angle 15°. The corresponding decrease of the transmission coefficient for a glass sample reached 15% for northwest direction against 24.8% for north direction after dust exposure period 70 of days. This dependence is related to the weather conditions including rain and wind. Another paper [5] studied the effect of dust accumulation-period on the PV modules surface and found output power loss by about 28% with dust accumulation continued up 60 days without cleaning. In a previous research work, the loss of efficiency reached up to 35–40% within several months [6] due to dust accumulation. The average degradation due to dust accumulation was accordingly around 6.2, 11.8, and 18.7% for the exposure periods of 1 day, 1 week, and 1 month [7].

PV modules are shaded not only by dust accumulation but also by bird drops, wildlife, passing clouds, buildings, trees, or other radiation blocking objects in proximity to PV modules. The power dissipation in the shaded cell(s) increases the cell temperature and eventually may create hot spots. Consequently, the entire PV system performance in terms of energy production and lifetime is degraded. The shading effect on an individual cell reflects itself on changing the cell parameters, e.g., the shunt and series resistance and the shaded cell(s) become reverse biased to serve as a load instead of a generator. Most of the researchers studied the electrical parameters of clean and dusty PV modules

as influenced by solar radiation, air humidity, wind speed, ambient temperature, and module cell temperature. The effect of dust accumulation, water droplets, birds' droppings, and partial shading conditions on the performance of a PV module was investigated experimentally [8].

A research paper studied different factors affecting dust accumulation on the surface of a PV module such as the number of exposure days of PV modules to the outdoor-dust environment, different tilt angles of PV modules, location of PV modules, type of dust, and the dust deposition density [9].

The impact of dust accumulation on the PV module output power was reviewed [10] being influenced by wind, relative humidity, and temperature where the module is located. This makes it possible to characterize the dust-collected in different countries as regards its generation, properties, and particle size. The decay of the PV module output current, voltage, and power with the increase of dust accumulation in (g m^{-2}) was recorded [11] experimentally in urban, agriculture, desert, and marine regions in Iraq.

The current–voltage characteristic curve of a dusty PV module being represented by a single-diode model was determined [12] based on the module equivalent circuit with four parameters after excluding either the series or parallel resistance from the circuit. The effect of dust on the I-V characteristic of the module was studied not only at STC but also at NOCT condition.

The influence of dust deposition on module surface was found [13] to affect significantly the short-circuit current and maximum power output of PV module with less effect on open-circuit voltage. This conforms to the findings reported before [14] where the dust deposition decreases the short-circuit current more than that of the open-circuit voltage. The percentage decrease of the short-circuit current reached 21.47% compared to less than 1% for the open circuit voltage after exposure to dust for a period of 70 of days to end up with dust deposition density of 6.09 g m^{-2}. The rate of performance degradation strongly depends on the mass of deposited dust particles on the module [13] and on the tilt angle and orientations of the PV modules [15].

Some literature studied how the performance of PV modules is influenced by dust accumulation on the surface of a module located in Middle East and North Africa region as well as the Far East region [16] in Sahara environment [17] and in the region of the East Bank of the Nile [18].

Tracking the solar radiation through the layers of a clean PV module [19, 20] and through the layers of a dusty module with uniform distribution of dust on the surface was followed [21] to calculate the total transmittance and reflectance. The error in calculating the total transmittance and reflectance reached 17% and 12%, respectively.

The propagation of solar radiation through a set of layers simulating those of a PV module was investigated [22]. A study was aimed at assessing the increase of power loss through the layers of a PV module exposed to solar radiation with the increase of the number of module layers [23].

Prediction of solar PV electrical output under variable experimental conditions was reported [24]. Modified semiempirical correlations to predict how the transmission coefficient of radiation through a PV module is influenced by surface deposition of dust. Of course, the application range of these correlations is limited. The dependence of the loss of current, output voltage, and cell temperature on dust accumulation on the surface

of a PV module was investigated. This motivates the present authors to study how the solar radiation propagates through the different layers of a PV module in order to evaluate the transmission coefficient through a proposed computer algorithm with no need for conducting experiments, which may be expensive. The algorithm is based on the optical properties of the surrounding air, the surface dust layer, and the glass cover of the PV module.

The present work is aimed at modelling PV modules taking into consideration the dust accumulation on the module surface. Thus, the dusty PV module consists of three layers; namely, ambient air, dust layer, and glass cover of the solar cell. These layers are named layers (0), (1), and (2) as shown in Fig. 1.

The energy of solar radiation is attenuated due to its passage through the three layers of the module. One of the targets to express the novelty of the present work is to assess how the intensity of solar radiation is reduced by the presence of accumulated dust on the PV module with no need for experiments, which may be expensive. This calls for a method to follow-up of the incident solar radiation during its reflection and transmission at the interfaces between layers and absorption through the dust layer and the glass cover. The method is based on optical properties of air, dust, and glass. This makes it possible to evaluate the parameters of the module, which appear in the equivalent circuit of the dusty module.

This paper is organized as follows: "Introduction" section is assigned for the introduction. "Research gaps" section is devoted to express the novelty of the present work by outlining the research gaps to be investigated in the paper. "Materials and methods" section with title "Materials and methods" including a proposed methodology to follow up the propagation of solar radiation through a dusty PV module, characterization of the accumulated dust, and calculation of I-V characteristic of PV module as influenced by dust accumulation as well as description of the experimental setup and technique to support experimentally the theoretical findings. Results and discussions are reported in "Results and discussions" section, and finally, a conclusion is presented in "Conclusion" section.

Research gaps

The novelty of the present work lies in proposing a method for the first time to follow-up the penetration of solar radiation through the different layers of a dusty module including the surrounding air, the dust layer, and the glass cover. The dust layer is deposited

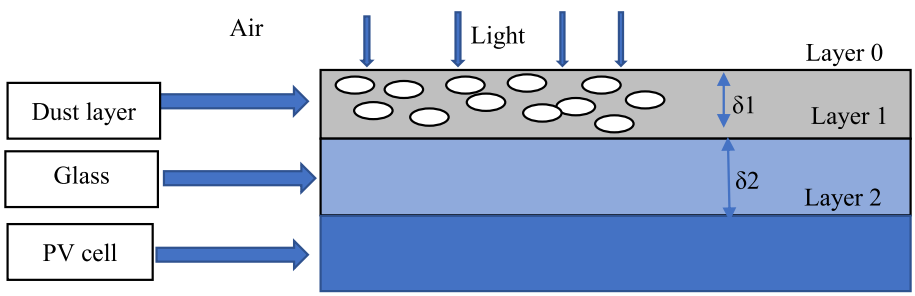

Fig. 1 PV module consists of three layers

naturally from the surrounding atmosphere. The method is aimed at evaluating the intensity of radiation received by the module after penetration through the module layers with no need for conducting experiments, which may be expensive. The method is based on optical properties of air, dust, and glass. This makes it possible to evaluate the parameters of the module, which appear in the equivalent circuit of the dusty module. This is in addition to evaluate the datasheet values as influenced by the presence of dust on the module surface.

Materials and methods

Proposed methodology to follow-up incident radiation through the PV module

Figure 2 shows a dusty PV module exposed to solar radiation with intensity G. The module is composed of three layers; namely, air, dust, and glass. The computer code built to follow-up the incident radiation through the layers of the module is described as follows:

- At point a, the incident radiation G experiences reflection in air along the direction ab with intensity Gr_{10} and transmission along the direction ac in dust with intensity Gt_{01} at a and intensity $Gt_{01}e^{-\alpha_1\delta_1}$ at c where α_1 and δ_1 are the absorption coefficient and thickness of the dust layer. r_{10} is the reflectance between layer 1 (dust layer) and layer 0 (ambient air). t_{01} is the transmittance between layer 0 and layer 1.
- At point c, the incident radiation along ac experiences reflection in dust along the direction cd with intensity $Gt_{01}e^{-\alpha_1\delta_1}r_{21}$ and transmission along the direction ce in glass with intensity $Gt_{01}e^{-\alpha_1\delta_1}t_{12}$ at c and intensity $Gt_{01}e^{-(\alpha_1\delta_1+\alpha_2\delta_2)}t_{12}$ at e where α_2 and δ_2 are the absorption coefficient and thickness of the glass layer. r_{21} is the reflectance between layer 2 (glass cover) and layer 1. t_{12} is the transmittance between layer 1 and layer 2.

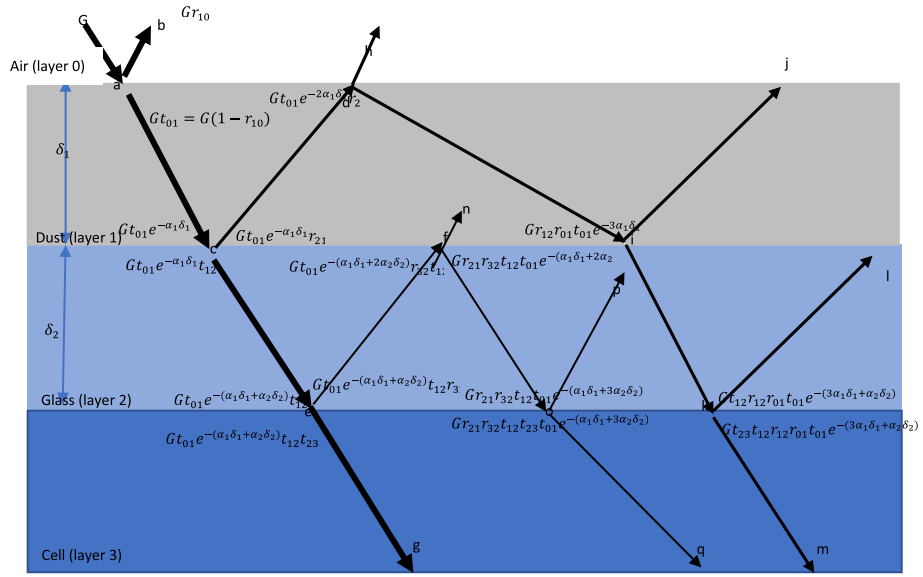

Fig. 2 Follow-up of incident radiation with reflection and transmission through the three layers of the dusty PV module ▬ Propagation through the 3 layers of the module. —— Propagation through dust layer no. 1. ——— Propagation through glass layer no. 2

- At point *e*, the incident radiation along ce experiences reflection in glass along the direction ef with intensity $Gt_{01}e^{-(\alpha_1\delta_1+\alpha_2\delta_2)}t_{12}r_{32}$ and transmission to be received by the surface of the PV cell with intensity $Gt_{01}e^{-(\alpha_1\delta_1+\alpha_2\delta_2)}t_{12}t_{23}$. r_{32} is the reflectance between surface of the PV cell and layer 2. t_{23} is the transmittance between layer 2 and layer 3.
- The reflected radiation in the direction cd experiences at d, j,.. reflection in dust and transmission in air as well as reflection in dust and transmission in glass at i,…
- The reflected radiation in the direction of experiences at f, i,.. reflection in glass and transmission in dust as well as reflection in dust and transmission into the surface of the PV cell at o, k, …
- The radiation received by the solar module is $Gt_{01}e^{-(\alpha_1\delta_1+\alpha_2\delta_2)}t_{12}t_{23} + Gr_{21}r_{32}t_{12}t_{23}t_{01}e^{-(\alpha_1\delta_1+3\alpha_2\delta_2)} + Gt_{23}t_{12}r_{12}r_{01}t_{01}e^{-(3\alpha_1\delta_1+\alpha_2\delta_2)}$

Of course, the radiation received by the module is less than the incident one, which decays due to its propagation through the module layers.

Characterization of the accumulated dust

Assumptions

The dust is assumed uniformly distributed over the surface of the module in the light of the fact that of Assiut City (27.17°, 31.19°), where the module is installed in atmosphere free from wind and rain.

Determination of reflectance and transmittance at the interface between layers as well as layer absorption coefficient

The reflectance $r_{\updownarrow,j}$ and transmittance $t_{\updownarrow,j}$ were expressed [21] at the interface between two-layer media $\updownarrow$ and j in touch as follows:

$$r_{\updownarrow,j} = \frac{(n_{\updownarrow} - n_j)^2 + (k_{\updownarrow} - k_j)^2}{(n_{\updownarrow} + n_j)^2 + (k_{\updownarrow} + k_j)^2} \tag{1}$$

$$t_{\updownarrow,j} = 1 - r_{\updownarrow,j} \tag{2}$$

In another approach, the reflectance $r_{\updownarrow,j}$ was expressed as follows [19, 20]:

$$r_{\updownarrow,j} = \frac{(n_{\updownarrow} - n_j)^2}{(n_{\updownarrow} + n_j)^2} \tag{3}$$

The subscript $\updownarrow$ j means that the radiation travels from layer $\updownarrow$ to layer j. $n_{\updownarrow}$ and $k_{\updownarrow}$ are the refractive and absorption indices of the $\updownarrow^{th}$ layer. n_j and k_j are the same for the j^{th} layer. The indices of the dust layer depend on the wavelength of the imposed radiation.

It is worthy mention that *n* and *k* values are known in the literature for ambient air (layer 0) and glass cover (layer 2) in Fig. 1. However, *n* and *k* for the dust sample (layer 1) are unknowns and depend on the type of dust, being determined by the installation site of the PV module.

The absorption coefficient α for the dust and glass layers is calculated in terms of the absorption index k at a given wavelength λ of the incoming radiation using the following equation [21, 25]:

$$\alpha(\lambda) = \frac{4\pi \mathrm{k}}{\lambda} \tag{4}$$

Determination of indices n_{eff}, k_{eff}, and α_{eff} of the dust sample as a whole

The absorption index k of the dust where exposed to radiation of a wavelength λ is obtained by applying volume fraction (percentage) [21] for all constituents of the dust sample as expressed by the following equation:

$$\mathrm{k}(\lambda) = \sum_{\mathrm{i}} \mathrm{f_{v,i}} \mathrm{k_i} \tag{5}$$

where k_i and $f_{\mathrm{v,i}}$ represent the absorption index k at wavelength λ and the volume fraction f_v of the i^{th} dust constituent.

The refractive index n of the dust when exposed to radiation of a wavelength λ is also obtained by applying volume fraction (percentage) [26] for all constituents of the dust sample as expressed by the following equation:

$$\mathrm{n}(\lambda) = \sum_{\mathrm{i}} \mathrm{f_{v,i}} \mathrm{n_i} \tag{6}$$

where n_i is the refractive index of i^{th} dust constituent at wavelength λ.

The effective values of n_{eff}, k_{eff}, and α_{eff} for all dust sample when exposed to solar radiation with a useful range of wavelength λ (from 0.21 to 1.1 μm) and α_{eff} are obtained as follows:

$$n_{\mathrm{eff}} = \left(\sum_{\lambda=0.21}^{1.1} \mathrm{n}(\lambda)\right)/\mathrm{M} \tag{7}$$

$$k_{\mathrm{eff}} = \left(\sum_{\lambda=0.21}^{1.1} \mathrm{k}(\lambda)\right)/\mathrm{M} \tag{8}$$

$$\alpha_{\mathrm{eff}} = \left(\sum_{\lambda=0.21}^{1.1} \alpha(\lambda)\right)/\mathrm{M} \tag{9}$$

where M is the number of selected wavelengths in the range from 0.21 to 1.1 μm.

Determination of density for the dust sample

The density of mixed dust constituents ρ is calculated in terms of volume fraction (percentage) [21].

$$\rho = \sum_{\mathrm{i}} \mathrm{f_{v,i}} \rho_\mathrm{i} \tag{10}$$

where ρ_i and $f_{\mathrm{v,i}}$ represent the density ρ and the volume fraction (percentage) $\mathrm{f_v}$ of the i^{th} dust constituent.

In another approach, the reciprocal of the dust density ρ^{-1} was calculated in terms of mass fraction (percentage) [27] as follows:

$$\rho^{-1} = \sum_{i} \frac{f_{m,i}}{\rho_i} \tag{11}$$

where $f_{m,i}$ represent the mass fraction (percentage) f_m of the i^{th} dust constituent.

Equation (10) serves in calculating n and k of the dust sample [27] as a whole as expressed by the following equation:

$$n(\lambda) = \rho \sum_{i} \frac{f_{m,i}}{\rho_i} n_i \tag{12}$$

$$k(\lambda) = \rho \sum_{i} \frac{f_{m,i}}{\rho_i} k_i \tag{13}$$

Determination of thickness for the dust sample

The thickness δ_1 of the deposited dust layer (layer no. 1 in Fig. 1) on the module surface is calculated as follows:

$$\delta_1 = \frac{m}{\rho A} \tag{14}$$

where m and ρ are the mass of the accumulated dust over the module surface area A and density of the dust, respectively.

Calculation of I-V characteristic of PV module as influenced by dust accumulation

The PV module is represented by an equivalent circuit, Fig. 3, which consists of a photogenerated current source and a shunt diode as well as series and parallel resistors. The parameters of the equivalent circuit are five including photon current source I_{ph}, diode reverse saturation current I_0, diode ideality factor A, series contact resistance R_s, and parallel leakage resistance R_p. The parameters are determined [28, 29] according to the datasheet values provided by modules' manufacturer. The datasheet information refers to the standard test condition (STC) with $1000 W/m^2$ solar irradiance, 25 °C cell

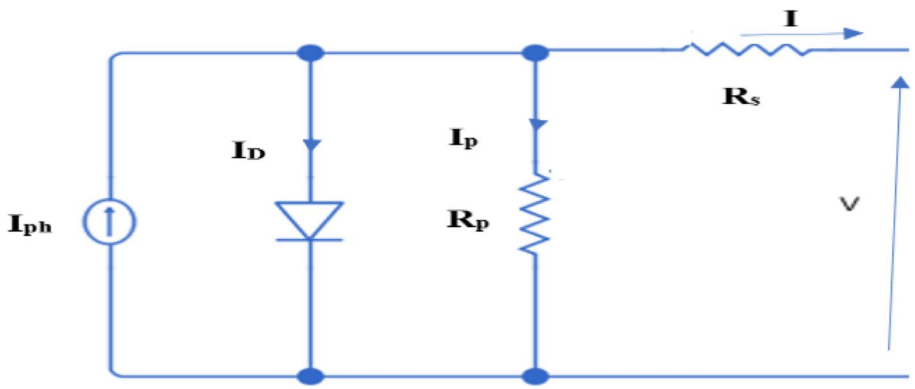

Fig. 3 Equivalent circuit of a PV module. I_{ph}, photon current source. I_D, diode current. R_p, parallel leakage resistance. R_s, series contact resistance

temperature, and 1.5 air-mass ratio (AM). Some manufacturers also give coefficients k_v, k_p, and k_i to account for the variations of V_{oc}, P_{mpp}, and I_{sc} current with cell temperature.

According to the equivalent circuit of a PV module, the current–voltage relationship at a specified irradiation G and cell temperature T is expressed as follows:

$$I = I_{ph} - I_0\left[e^{\frac{q(V+R_sI)}{NAkT}} - 1\right] - \frac{V + R_sI}{R_p} \tag{15}$$

where I and V are the module output voltage and current, k is Boltzmann's constant (1.38×10^{-23} J/K), q is the electron charge (1.6×10^{-19} C), and T is the cell temperature in kelvin (K).

On changing the operating condition of the PV module different from the STC condition, the datasheet values have to be changed according to the solar radiation G in W/m^2 and cell temperature T in °k.

The cell temperature T is related to the ambient temperature T_a by the following equation:

$$T = (T_{noct} - 25) \times \frac{G}{800} + T_a \tag{16}$$

where T_{noct} is the normal operating cell temperature (usually given in module datasheet).

The module parameters I_{ph}, I_0, R_p, R_s, and A are obtained from datasheet at STC and corrected [30] using k_v, k_i, andk_p (from datasheet) according to the radiation G received by the dusty module and cell temperature being dependent on ambient temperature T_a. as expressed by Eq. (16). The datasheet values are also corrected according to G and T_a as follows:

$$I_{sc} = I_{sc,STC} \times \left(\frac{G}{G_{STC}}\right)[1 + k_i \times (T - 25)] \tag{17}$$

$$V_{oc} = V_{oc,STC} \times [1 + k_v \times (T - 25)] \tag{18}$$

$$I_{mpp} = I_{mpp,STC} \times \left(\frac{G}{G_{STC}}\right)[1 + k_i \times (T - 25)] \tag{19}$$

$$V_{mpp} = V_{mpp,STC} \times (1 + k_v \times (T - 25)) \tag{20}$$

Of course, the solar radiation G in Eqs. (17), (18), (19) and (20) is different from the incident one due to the presence of dust on the module surface. The dust accumulation on the PV module surface reduces strongly the optical transmissivity of the module. Consequently, a corresponding degradation in the module's performance is evaluated through the so-called dust degradation factor (DDF) which is defined as follows [31].

$$DDF\% = \left[\frac{F_{PVc} - F_{PVd}}{F_{PVc}}\right] \times 100 \tag{21}$$

where F_{PVc} and F_{PVd} are the parameters of the PV clean the dusty modules.

The – I-V characteristic curve is obtained using Eq. (15) with the determined parameters of the equivalent circuit.

Experimental

Experimental setup

The experimental setup includes the following components:

1. Two PV modules (LC175-24 M, LORENTZ, Germany) installed on the roof of the electrical engineering department building of Assiut University as shown in Fig. 4; one module is exposed to dust, and the other is kept clean from dust by manual cleaning with water using cloth and squeegee before starting the measurements.
2. Connecting cables from the PV module at the building rooftop to an indoor laboratory in the basement of the building.
3. X-ray fluorescence (XRF) device for dust analysis and SEM (scanning electron microscope) for particle-size characterization
4. Voltmeter and ammeter meters for measuring load voltage V and cell current I.
5. Variable load resistance for changing the cell current I.

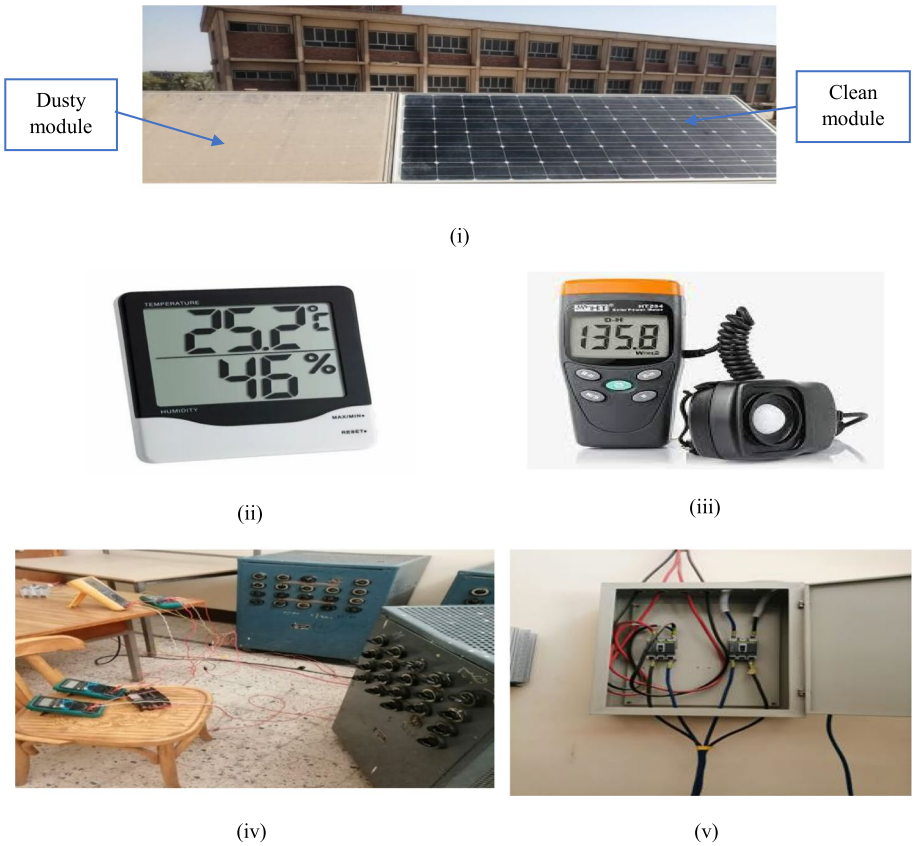

Fig. 4 Set up components for measuring I-V characteristic of the PV module. (i) Two PV modules on the roof on of EE Department. (ii) Digital TFA Thermo Hygrometer for measuring ambient temperature. (iii) HT 204 solar power meter for measuring solar radiation. (iv) Voltmeter and ammeter instruments for measuring load voltage V and cell current of the PV module + variable load resistances to change the output current. (v) Cable extended from rooftop to indoor laboratory where measuring equipment (iv) is located

6. Digital balance for weighing the collected dust.
7. Ambient temperature sensor (Digital TFA Thermo-Hygrometer, Scipro Technologies, India).
8. Incident solar-radiation meter (HT 204 solar power meter, Italy) for measuring solar radiation. The radiation values are also quoted from previous measurements of solar radiation in Assiut City as reported before http://enerwin.com/enerwin/; https://www.trnsys.com.

Table 1 lists the used devices including the thermo-hygrometer, solar power meter, digital balance, voltmeter, and ammeter as well as their respected accuracy, resolution, and measuring range.

Technique

The experimental methodology for assessing indices (n) and (k) of the accumulated dust on the PV module is explained as follows:

1. Collect the accumulated dust on the module from its all-surface area after 3-month exposure period (from June 2022 to September 2022) and weigh the collected dust using the digital balance.
2. Analyze the dust using X-ray fluorescence (XRF) apparatus to assess the constitutes of the dust and use SEM device for particle-size characterization.
3. Afterwards, the dusty module was cleaned manually by using a brush, cloth, and hand high-pressure water spray from a hose [16, 32].
4. Calculate the thickness of the deposited dust layer on the module using Eqs. (10) and (14).
5. Identify constituents of the collected dust and convert mass percentages into volume fractions (percentages).
6. Quote n and k for each constituent of the dust at different values of radiation-wavelength λ from published work in the literature.
7. Calculate n and k of the dust sample using Eqs. (5) and (6) for each wavelength over the useful wavelength-range λ of the solar radiation. Then, the effective values of n_{eff}, k_{eff} and α_{eff} are calculated using Eqs. (7), (8), and (9).

Table 1 List of used devices as well as their respected accuracy, resolution, and measuring range

Devices	Accuracy	Resolution	Range
Digital TFA Thermo-Hygrometer	± 1.0 °C & F and ± 2% mid-range ± 4% elsewhere	0.1 temperature and 1.0% relative humidity	− 14 to + 140 °F (− 10 to + 60 °C)
HT 204 solar power meter	> between ± 10 W/m^2 and ± 5% rdg and ± 0.38 W/m^2/°C from 25 °C	1 W/m^2	1–1999 W/m^2
ViBRA SJ-6200 Precision Digital Balance	-	0.1 g	6200–0.1 g
Voltmeter	± 0.6% rdg ± 4dgt ± 1.0% rdg ± 4dgt	-	400 mV/4 V/40 V/400 V 600 V
Ammeter	± 2.0% rdg ± 4dgt ± 1.0% rdg ± 4dgt ± 1.6% rdg ± 4dgt	-	400 µA/4000 µA 40 mA/400 mA 4 A/10 A

The effective values of indices (n) and (k) of dust as well as the corresponding known values for air and glass represent the input data of the computer code to evaluate the reflectance and transmittance at the interface between the different layers of the PV module and the absorption coefficient of the dust layer and glass cover. This ends up with the evaluation of the percentage of the incident radiation G that reaches the surface of the dusty PV module.

Results and discussion

Analysis of dust samples

The X-ray fluorescence identified 23 constituents of the dust sample, namely, F, Na2O, MgO, Al2O3, SiO2, P2O5, SO3, Cl, K2O, Cao, TiO2, V2O5, Cr2O3, MnO, Fe2O3, NiO, CuO, ZnO, SrO, ZrO2, PbO, LOI-HCNO, and S-BLEN. The mass percentage of the constituents is given in Table 2.

Ten constituents SiO2, Cao, MgO, Al2O3, Fe2O3, TiO2, F, P2O5, SO3, and bird dropping (LOI-HCNO) are selected from Table 2, whose mass percentage is high compared to other constituents.

Six of the ten selected constituents SiO2, Cao, MgO, Al2O3, Fe2O3, and TiO2 have known n and k values, which depend on the wavelength of the radiation [21]. For the remaining four constituents F, P2O5, SO3, and bird dropping, the n value is assumed constant independent of the wavelength with respective values 1, 1.436, 1.4097, and 1.485 http://wwww.microlabgallery. Because their k values are not an available in the literature, they are assumed equal to zero in the light of their small values.

One of the SEM images of the accumulated dust particles on the surface of the module is shown in Fig. 5. The size of the dust particles varied in the range from 0.22854 to 16.49887 μm, exhibiting mean size of 0.64687 μm. The range of particle size conforms to those reported before [10] for a size range of 0.5–780 μm [17], for a size range of 0.5–1000 μm, and [7] for a size range of 0.3–1.2 μm.

Table 2 Main constituents of the dust sample by XRF

No	Constituents of the dust sample		Mass percentage (%)	No	Constituents of the dust sample		Mass percentage (%)
1	Fluorine	F	2.0258	13	Chromium oxide nanopowder	Cr2O3	0.0249
2	Sodium oxide	Na2O	1.3399	14	Manganese(II) oxide	MnO	0.1363
3	Magnesium oxide	MgO	2.379	15	Iron(III) oxide	Fe2O3	6.2732
4	Aluminum oxide	Al2O3	7.9898	16	Nickel(II) oxide	NiO	0.1464
5	Silicon Dioxide	SiO2	25.675	17	Copper oxide	CuO	0.0123
6	Phosphorus pentoxide	P2O5	2.1182	18	Zinc oxide	ZnO	0.0561
7	Sulfur trioxide	SO3	7.0933	19	Strontium oxide	SrO	0.0704
8	Chlorine	Cl	0.4032	20	Zirconium dioxide	ZrO2	0.0266
9	Potassium oxide	K2O	1.3111	21	Lead(II) oxide	PbO	0.0253
10	oxide crystallizes	Cao	20.6894	22		LOI-HCNO	20.804
11	Titanium dioxide	TiO2	1.0625	23		S-BLEND	0.0848
12	Vanadium pentoxide	V2O5	0.3384				

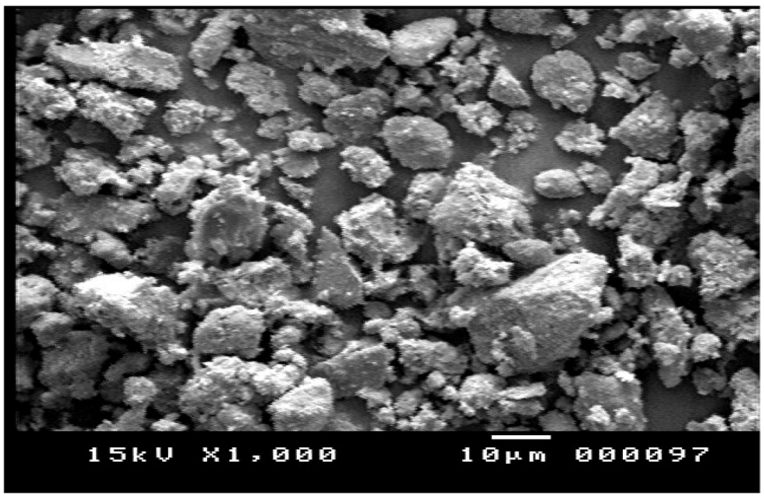

Fig. 5 SEM image of particles' size in the dust sample

Table 3 Conversion of mass percentages into volume fractions of the main constituents of the dust to serve in calculating the density of the dust sample

No	Constituents of the dust sample	Mass%	Density (g/cm^3)	Volume percentage (%)	$f_{v,i}\rho_i$
1	F	2.0258	1.696	2.175367	0.0369
2	Na2O	1.3399	2.27	1.075	0.024406
3	MgO	2.379	3.58	1.210245	0.043333
4	Al2O3	7.9898	3.7	3.932746	0.145534
5	SiO2	25.675	2.29	20.41911	0.467668
6	P2O5	2.1182	2.39	1.614101	0.038583
7	SO3	7.0933	1.92	6.728354	0.129204
8	Cl	0.4032	3.2	0.229473	0.007344
9	K2O	1.3111	2.32	1.029223	0.023882
10	Cao	20.6894	3.35	11.24773	0.376856
11	TiO2	1.0625	4.23	0.457457	0.019353
12	V2O5	0.3384	3.36	0.183423	0.006164
13	Cr2O3	0.0249	5.21	0.008704	0.000454
14	MnO	0.1363	5.43	0.045715	0.002483
15	Fe2O3	6.2732	5.24	2.180317	0.114266
16	NiO	0.1464	6.67	0.039974	0.002667
17	CuO	0.0123	6.32	0.003544	0.000224
18	ZnO	0.0561	5.61	0.018212	0.001022
19	SrO	0.0704	4.7	0.02728	0.001282
20	ZrO2	0.0266	5.56	0.008713	0.000485
21	PbO	0.0253	9.53	0.004835	0.000461
22	LOI-HCNO	20.804	0.8	47.36075	0.378944
23	S-BLEND	0.0848			
				$\sum_i f_{v,i}\rho_i = 1.821514$	

Table 3 gives conversion of mass percentage of the main constituents of the dust into volume fractions (percentages) [21] along with the product of both f_v and ρ for each i^{th} constituent. This makes it possible to calculate n and k indices of the dust

sample using Eqs. (5) and (6) as well as the sample density according to Eq. (10). This ends up with a density value of 1.82 g/cm^3 for the investigated dust sample.

Figure 6 is obtained according to the following steps:

1. For each wavelength, the refractive and absorption indices n and k are calculated for each selected constituent of the dust sample in the range 0.21–1.1 μm.
2. For each wavelength, n and k are determined for the dust sample as a whole using Eqs. (5) and (6). The absorption coefficient α is determined using Eq. (4).
3. Effective values of n_{eff}, k_{eff}, and α_{eff} of the dust sample for all wavelengths are determined using Eqs. (7), (8) and (9).

The steps 1–3 are aimed at evaluating the solar radiation that will be received by the module after its penetration through the module layers including the dust sample and glass cover.

The effective values n_{eff}, k_{eff}, and α_{eff} are equal to 1.525, 2.43×10^{-3}, and 5.11×10^{-2}, respectively, with the number M of selected wavelengths over the range from 0.21 to 1.1 μm is equal to 90. The results showed that the received radiation is less than the incident one with a subsequent loss in the module output power.

It is quite clear that the value of n_{eff} agreed reasonably with those reported in the literature, where n_{eff} was quoted from AERONET network of ground-based radiometers to record values in the range from 1.48 to 1.56 [33] and values from 1.35 to 1.65 [34] and a constant value equal to 1.53 [34, 35].

It is quite clear that the value of k_{eff} agrees reasonably with those reported in the literature, where k was measured for five dust samples [34]: one sample from Egypt, three samples from Morocco, and one sample from West Africa. The range of k at different wavelengths was found to vary over the range $(2.1 - 15.7) \times 10^{-3}$ in Egypt, $(2.9 - 22) \times 10^{-3}$ in Morocco, and $(2.4 - 49.5) \times 10^{-3}$ in West Africa at wavelength from 0.3 to 0.955 μm. The range of k was found to vary over the range

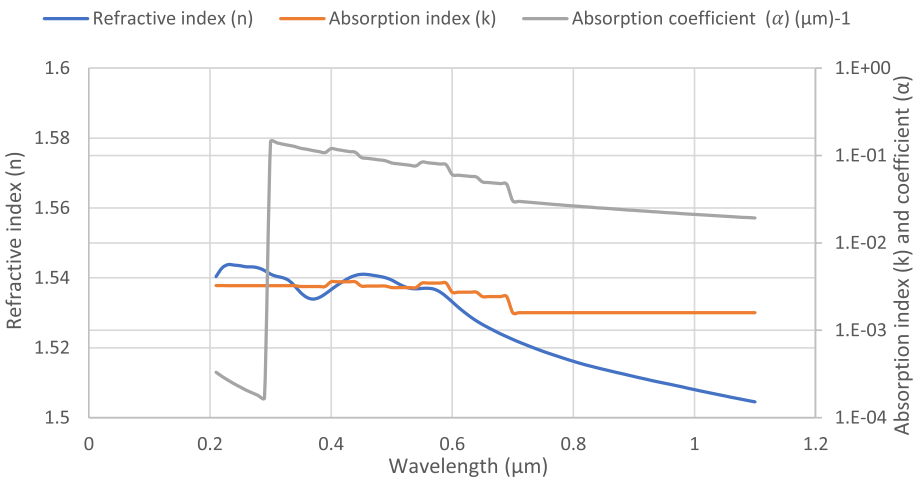

Fig. 6 Refractive index (n), absorption index (k), and absorption coefficient (α) of dust sample as influenced by wavelength of solar radiation

Table 4 Datasheet values of LC175-24 M PV module http://www.tehnosat.ro/PVmodules/lorentz_LC175-24M

All technical data at standard test condition: $AM = 1.5$, $G = 1000\ W/m^2$, cell temperature $T = 25\ °C$			
Peak power Pmax [Wp]	175 + 10% /–5%	Temperature coefficient for Pmax [%/°C]	−0.50
Max. power current Imp [A]	5.0	Temperature coefficient for Voc [%/°C]	−0.35
Max. power-voltage Vmp [V]	35.0	Temperature coefficient for Isc [%/°C]	0.09
Short circuit current Isc [A]	5.4	Number of cells in series	72
Open circuit voltage Voc [V]	44.4	Number of cells in parallel	1
Dimension [mm] 808 × 1,580 × 35			

Table 5 Corrected datasheet values and corresponding module parameters at $T_a = 44\ °C$ and $G_{incident} = 1027\ W/m^2$

Clean PV module at $T_{cell} = 74\ °C$ and $G = 1027\ W/m^2$ http://enerwin.com/enerwin/		**Dusty PV module at $T_{cell} = 64\ °C$ and $G = 702\ W/m^2$ http://enerwin.com/enerwin/**		DDF%	
Corrected datasheet values	**Corresponding module parameters**	**Corrected datasheet values**	**Corresponding module parameters**	**Datasheet values**	**Module parameters**
$I_{mpp} = 4.9107$	$I_{ph} = 5.3078$	$I_{mpp} = 3.386$	$I_{ph} = 3.8881$	$I_{mpp} = 31.04853$	$I_{ph} = 26.74743$
$V_{mpp} = 29.756$	$I_0 = 3.545e\text{-}05$	$V_{mpp} = 29.59$	$I_0 = 7.519e\text{-}06$	$V_{mpp} = 0.557871$	$I_0 = 78.78984$
$P_{mpp} = 179.4758$	$R_s = 0.0139$	$P_{mpp} = 123$	$R_s = 0.0139$	$P_{mpp} = 31.46708$	$R_s = 0$
$I_{sc} = 5.3036$	$R_p = 10.9831$	$I_{sc} = 3.6569$	$R_p = 16.069$	$I_{sc} = 31.04872$	$R_p = -46.3066$
$V_{oc} = 36.9081$	$A = 1.4387$	$V_{oc} = 37.633$	$A = 1.3999$	$V_{oc} = -1.96407$	$A = 2.696879$

$(2.08 - 4.62) \times 10^{-3}$ in Oman and $(2.5 - 5.7) \times 10^{-3}$ in United Arab Emirates at wavelength from 0.3 to 0.7 μm [21].

The values of the indices n and k are known in the literature for ambient air, glass, and solar cell as equal to $n_{air} = 1$, $k_{air} = 0$ [36], $n_{glass} = 1.53$, $k_{glass} = 2.5 \times 10^{-9}$ [37], and $n_{solarcell} = 3.43$ and $k_{solarcell} = 0.01896923$ [35]. The calculated values for the dust layer $n_{eff,dust}$ and $k_{eff,dust}$ are 1.525 and 2.43×10^{-3}, respectively. The calculated thickness of dust layer δ_1 is 2.5 μm as obtained from Eq. (14) based on assuming uniform distribution of dust over the whole surface area of the module. This is because the site location of the module is free from wind and rain during the test period. The thickness of glass layer δ_2 is 3.2 mm being quoted from the literature [21].

Measured against calculated I-V characteristic of the PV module

The PV module under investigation is LC175-24 M with electrical specifications quoted from the datasheet as given in Table 4.

As given in Table 5, the datasheet values of V_{oc}, I_{sc}, I_{mpp}, V_{mpp}, and P_{mpp} are corrected using previous measurement of solar radiation in Assiut http://enerwin.com/enerwin/ at solar radiation G of 1027 W/m^2 and cell temperature T_{cell} of 74 °C (corresponding to ambient temperature of 44 °C) using Eqs. (16), (17), (18), (19) and (20) in order to calculate the five parameters of the clean PV module. This is a prerequisite for calculating the I-V and P–V characteristics of the clean module. This measurement data almost coincides with those using measurement of solar radiation using HT204 solar radiation meter. Also, Table 5 includes corresponding data for dusty module with incident

radiation of 1027 W/m^2 that decrease as the module surface to be 702 W/m^2 at cell temperature T_{cell} of value 64 °C (corresponding to ambient temperature of 44 °C). Therefore, the cell temperature of clean module recorded a value of 74 °C against 64 °C for dusty module. This is because the radiation level received by the clean module is 1027 W/m^2 and decreased to 702 W/m^2 for the dusty module. This conforms to previous findings reported before [32, 38].

In Table 5, it is quite clear that the dust degradation factor DDF assumed a value of 31% corresponding to a decrease of the short-circuit current against − 2% corresponding to an increase of the open-circuit voltage. This conforms to previous results reported before [31]. Table 5 shows also that the DDF value recorded highest value for the diode reverse saturation current I_0 and lowest value for the ideality factor A provided that DDF is zero for the series resistance R_s.

As given in Table 6, the datasheet values of V_{oc}, I_{sc}, I_{mpp}, V_{mpp}, andP_{mpp} are corrected using previous measurements of solar radiation in Assiut https://www.trnsys.com at solar radiation G of 915 W/m^2 and cell temperature T_{cell} of 70 °C (corresponding to ambient temperature of 44 °C) using Eqs. (16), (17), (18), (19) and (20) in order to calculate the five parameters of the clean PV module. This is a prerequisite for calculating the I-V and P–V characteristics of the clean module. Also, Table 6 includes corresponding data for dusty module with incident radiation of 915 W/m^2 that decrease at the module surface to be 626 W/m^2 at cell temperature T_{cell} of value 62 °C (corresponding to ambient temperature of 44 °C). Therefore, the cell temperature of clean module recorded a value of 70 °C against 62 °C for dusty module. This is because the radiation level received by the clean module is 915 W/m^2 and decreased to 626 W/m^2. This conforms to previous findings reported before [32, 38].

In Table 6, it is quite clear that the dust degradation factor DDF assumed a value of 31% corresponding to a decrease of the short-circuit current against − 1.5% corresponding to an increase of the open-circuit voltage. This conforms to previous results reported before [31]. Table 6 shows also that the DDF value recorded highest value for the diode reverse saturation current I_0 and lowest value for the ideality factor A provided that DDF is zero for the series resistance R_s.

The present results in Tables 5 and 6 being extracted from Figs. 7, 8, 9, 10, 11 and 12 conclude that the decrease of I_{sc} due to dust deposition is much higher than the increase of V_{oc},

Table 6 Corrected datasheet values and corresponding module parameters atT_a= 44 °C and$G_{incident}$= 915 W/m^2

Clean PV module atT_{cell}= 70 °C and *G* = 915 W/m^2 https://www.trnsys.com		**Dusty PV module atT_{cell}= 62 °C and G = 626 W/m^2 https://www.trnsys.com**		DDF%	
Corrected datasheet values	**Corresponding module parameters**	**Corrected datasheet values**	**Corresponding module parameters**	**Datasheet values**	**Module parameters**
I_{mpp}= 4.3885 V_{mpp}= 29.2952 P_{mpp}= 159.9177 I_{sc}= 4.7395 V_{oc}= 37.1935	I_{ph}= 4.7433 I_0= 3.545e-6 R_s= 0.0139 R_p= 12.3275 *A* = 1.4253	I_{mpp}= 3.0229 V_{mpp}= 29.6674 P_{mpp}= 109.3 I_{sc}= 3.2648 V_{oc}=37.7461	I_{ph}= 3.2674 I_0= 6.084–06 R_s= 0.0139 R_p= 18.035 A = 1.3907	I_{mpp}= 31.11769 V_{mpp}= − 1.27052 P_{mpp}= 31.652344 I_{sc}= 31.1151 V_{oc}= − 1.48574	I_{ph}= 31.115447 I_0= − 71.6 R_s= 0 R_p= − 46.29893 A = 2.4427559

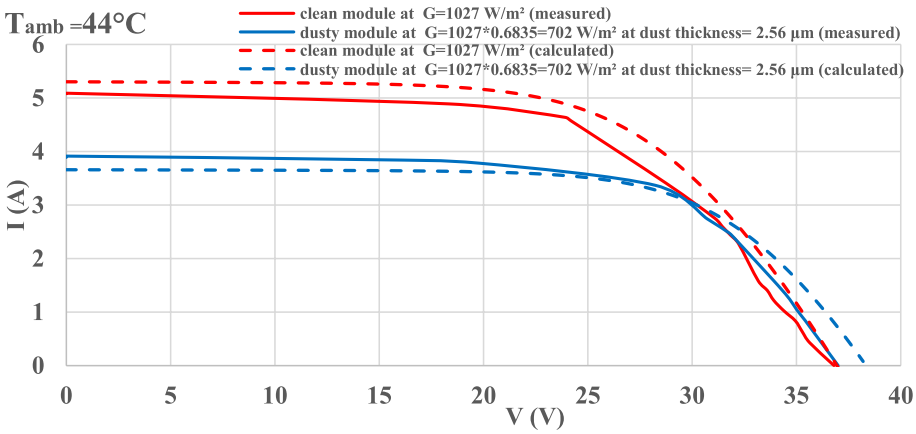

Fig. 7 Measured and calculated current–voltage characteristic curves of dusty and clean modules at ambient incident radiation of 1027 W/m^2 http://enerwin.com/enerwin/

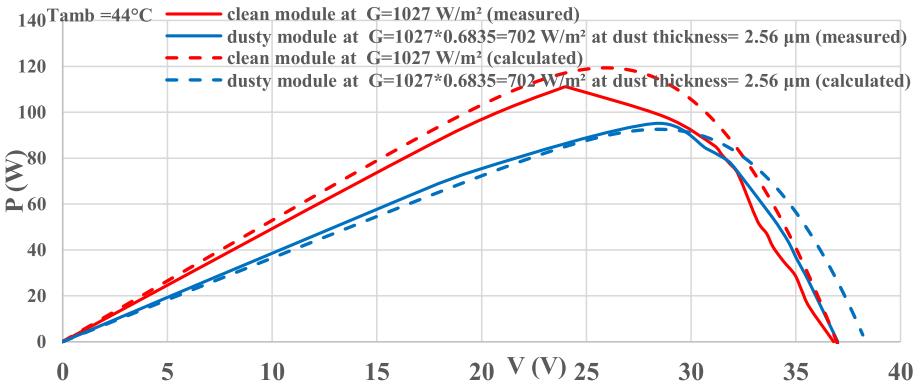

Fig. 8 Measured and calculated power-voltage characteristic curves of dusty and clean modules at ambient incident radiation of 1027 W/m^2 http://enerwin.com/enerwin/

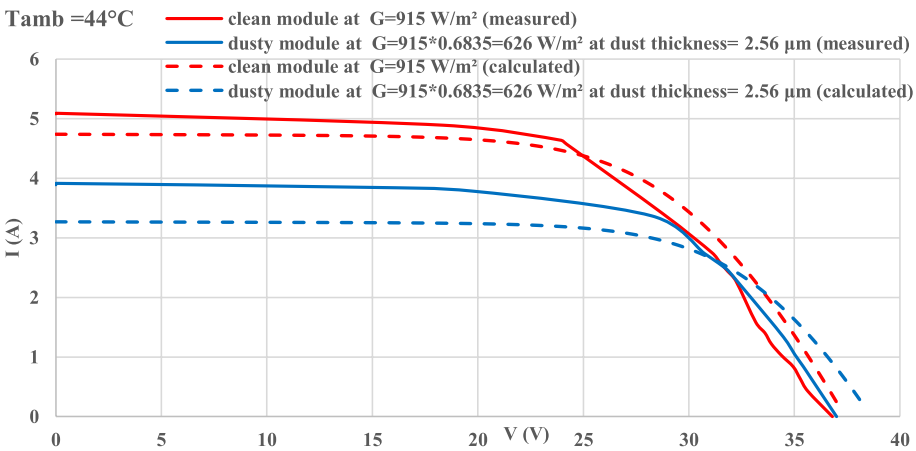

Fig. 9 Measured and calculated current–voltage characteristic curves of dusty and clean modules at ambient incident radiation of 915 W/m^2 https://www.trnsys.com

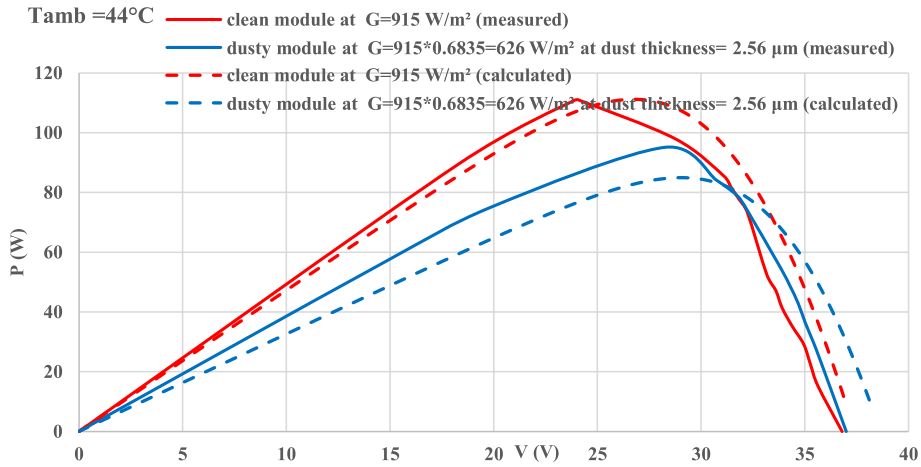

Fig. 10 Measured and calculated power-voltage characteristic curves of dusty and clean modules at ambient incident radiation of 915 W/m^2 https://www.trnsys.com

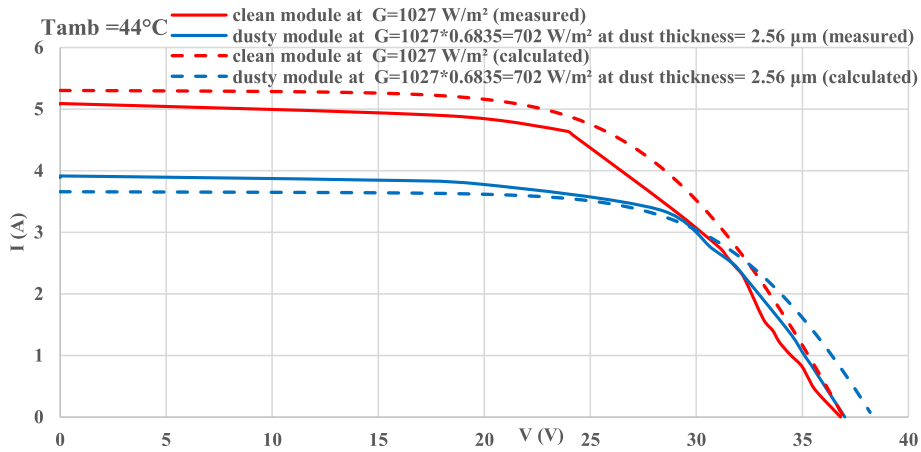

Fig. 11 Measured using HT204 solar radiation meter and calculated current–voltage characteristic curves of dusty and clean modules at measured ambient incident radiation of 1027 W/m^2

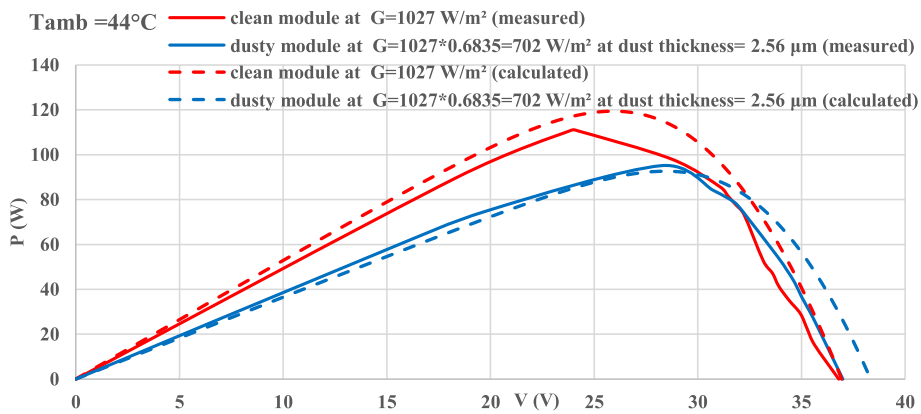

Fig. 12 Measured using HT204 solar radiation meter and calculated power-voltage characteristic curves of dusty and clean modules at measured ambient incident radiation of 1027 W/m^2

which conforms to previous findings published in the literature [31]. With the presence of dust on the module surface, the incident radiation decays due to its propagation through the module layers, so the intensity of received radiation is less than that of the incident one. This reflects itself on a decrease of I_{sc}. With the decrease of the radiation received by the module when compared with the incident one, the cell temperature decreases with a subsequent increase of V_{oc}. Of course, the increase of V_{oc} is very limited with respect to the decrease of I_{sc} [32, 38].

Figures 7 and 8 show the measured I-V and P–V curves of clean and dusty PV modules exposed to respective solar-radiation values G of 1027 and 702 W/m^2 (quoted from previous measurements recorded in Assiut City at the same day and hour http://enerwin.com/enerwin/) at cell temperature T_{cell} of 74 °C and 64 °C (determined by Eq. (16) corresponding to ambient temperature of 44 °C recorded by the temperature sensor). For comparison purpose, the calculated I-V and P–V curves of clean and dusty PV modules are shown in Figs. 7 and 8.

Figures 9 and 10 show the measured I-V and P–V curves of clean and dusty PV modules exposed to respective solar-radiation values G of 915 and 626 W/m^2 (quoted from previous measurements recorded in Assiut City at the same day and hour https://www.trnsys.com) at cell temperature T_{cell} of 70 °C and 62 °C (determined by Eq. (16) corresponding to ambient temperature of 44 °C recorded by the temperature sensor). For comparison purpose, the calculated I-V and P–V curves of clean and dusty PV modules are shown in Figs. 9 and 10.

Figures 11 and 12 show the measured I-V and P–V curves of clean and dusty PV modules exposed to respective solar-radiation values G of 1027 and 702 W/m^2 (measured by the portable solar radiation meter) at cell temperature T_{cell} of 74 °C and 64 °C (determined by Eq. (16) corresponding to ambient temperature of 44 °C recorded by the temperature sensor). For comparison purpose, the calculated I-V and P–V curves of clean and dusty PV modules are shown in Figs. 11 and 12. It is quite clear that the maximum output power of dusty module is less than that of the clean one by up to 31% confirming the effect of dust layer in reducing the radiation received by the module from 1027 to 702 W/m^2.

It is quite clear that the agreement between the calculated and measured I-V and P–V characteristics in Figs. 7, 8, 9, 10, 11 and 12 is satisfactory, and the difference between the calculated and measured characteristics lies within the experimental error of the used instruments. On the other hand, the satisfactory agreement between the calculated and measured characteristics confirms that the accuracy of both the procedure adopted for dust characterization and the computer code built to follow up the propagation of solar radiation through the layers of the dusty module.

It is worthy to mention that the I-V and P–V characteristics using previous measurements of solar radiation in Assiut http://enerwin.com/enerwin/ in Figs. 7 and 8 almost coincide with those in Figs. 11 and 12 using measurements of solar radiation using HT204 solar radiation meter at the same day and hour.

Conclusions

1. A method was proposed to follow up the incident radiation through a PV module considering the reflection and transmission of radiation at the interfaces between different module layers, namely, interfaces between (i) ambient-air and dust-layer, (ii)

dust-layer and glass-cover, and (iii) glass-cover and solar-cell surface. The absorption coefficient of radiation in the dust layer and glass cover was evaluated. The proposed method was formulated in a computer code.

2. The proposed method calls for determination of the reflectance and transmittance at the different interfaces as well as absorption coefficient of both the dust layer and the glass cover. Calculation of the reflectance and transmittance requests determination of the refractive index (n) and absorption index (k) for all module layers. The computer code was built to evaluate how the incident radiation is attenuated through the different module layers before reaching the solar cell.
3. Analysis of the accumulated dust was made to identify the dust constituents using X-ray fluorescence device (XRF). The n_i and k_i values were determined for each i^{th} constituent of the dust. Then, the *n* and *k* values of the dust sample as a whole were determined at each wavelength of the incident radiation depending on the volume fractions. This makes it possible to determine effective values n_{eff} and k_{eff} of the dust sample for all incident radiation. This is a prerequisite for the computer code. The values of n_{eff} and k_{eff} (1.525 and 0.00243) agreed reasonably with those reported in the literature.
4. With the determination of the radiation received by the PV module as well as the ambient temperature, the current–voltage characteristic of the dusty module was calculated using MATLAB Simulink with consideration of module parameters after being corrected according to the received radiation by the module and ambient temperature where the PV module was located. The intensity of received radiation depends on the type of dust and its thickness on the module surface.
5. The calculated current–voltage characteristic of the dusty module agreed reasonably with the measured one for 175-W PV module (LC175-24 M) where the incident radiation decreased to 68% due to dust accumulation after a period of 3 months. Such decrease of the radiation depends on the type of dust and its thickness over the module surface.
6. The accumulated dust decreased of the maximum output power of the dusty module by 31% when compared with the clean one. Such decrease of the radiation depends on the type of dust and its thickness over the module surface.
7. The decrease of short-circuit current I_{sc} recorded 31% due to dust deposition against 2% for the increase of open-circuit voltage V_{oc} at $T_a = 44$ °C and incident $G = 1027$ W/m^2. This conforms to findings reported in the literature which stated that the percentage decrease of I_{sc} due to dust deposition is much higher than the percentage increase of V_{oc}.

Acknowledgements
The authors would like to acknowledge Assiut University for PV modules on the roof of the EE department.

Authors' contributions
RK, methodology, software preparation, validation of software, investigation, and original draft writing. MA, methodology, investigation, and writing review and editing. MN, methodology, investigation, and draft writing. The authors read and approved the final manuscript.

Funding
The authors did not receive support from any organization for the submitted work, and no funds, grants, or other support was received.

Availability of data and materials
All presented data are available with the corresponding author under any request.

Declarations

Competing interests
The authors declare that they have no competing interests.

Received: 22 October 2022 Accepted: 10 February 2023
Published online: 21 February 2023

References

1. Middle East Solar Industry Association (2020) Solar Outlook Report: Dubai-UAE
2. New and Renewable Energy Authority (2018) Renewable energy outlook: Egypt
3. Jiang H, Lu L, Sun K (2011) Experimental investigation of the impact of airborne dust deposition on the performance of solar photovoltaic (PV) modules. Atmos Environ 45(25):4299–4304
4. Gholami A, Saboonchi A, Alemrajabi AA (2017) Experimental study of factors affecting dust accumulation and their effects on the transmission coefficient of glass for solar applications. Renew Energy 112:466–473
5. Benghanem M, Almohammedi A, Khan MT, Al-Masraqi A (2018) Effect of dust accumulation on the performance of photovoltaic panels in desert countries: a case study for Madinah, Saudi Arabia. Int J Power Electron Drive Syst 9(3):1356
6. Kazem HA, Chaichan MT (2016) Experimental analysis of the effect of dust's physical properties on photovoltaic modules in northern Oman. Sol Energy 139:68–80
7. Saidan M, Albaali AG, Alasis E, Kaldellis JK (2016) Experimental study on the effect of dust deposition on solar photovoltaic panels in desert environment. Renew Energy 92:499–505
8. Mustafa RJ, Gomaa MR, Al-Dhaifallah M, Rezk H (2020) Environmental impacts on the performance of solar photovoltaic systems. Sustainability 12(2):608
9. Styszko K, Jaszczur M, Teneta J, Hassan Q, Burzyńska P, Marcinek E, Łopian N, Samek L (2019) An analysis of the dust deposition on solar photovoltaic modules. Environ Sci Pollut Res 26(9):8393–8401
10. Khan RA, Farooqui SA, Khan MH, Sarfraz M, Luqman M, Khan M (2022) Dust deposition on PV module and its characteristics. The effects of dust and heat on photovoltaic modules: impacts and solutions. Springer, Cham, pp 59–95
11. Chaichan MT, Kazem HA, Al-Waeli AH, Sopian K (2020) The effect of dust components and contaminants on the performance of photovoltaic for the four regions in Iraq: a practical study. Renew Energy Environ Sustain 5:3
12. Gholami A, Ameri M, Zandi M, Ghoachani RG (2021) A single-diode model for photovoltaic panels in variable environmental conditions: investigating dust impacts with experimental evaluation. Sustain Energy Technol Assess 47:101392
13. Tripathi AK, Aruna M, Murthy CS (2017) Experimental investigation of dust effect on PV module performance. Glob J Res Eng 17(3):35–39
14. Gholami A, Khazaee I, Eslami S, Zandi M, Akrami E (2018) Experimental investigation of dust deposition effects on photo-voltaic output performance. Sol Energy 159:346–352
15. Babatunde AA, Abbasoglu S, Senol M (2018) Analysis of the impact of dust, tilt angle and orientation on performance of PV Plants. Renew Sustain Energy Rev 90:1017–1026
16. Shenouda R, Abd-Elhady MS, Kandil HA (2022) A review of dust accumulation on PV panels in the MENA and the Far East regions. J Eng Appl Sci 69(1):1–29
17. Mohamed AO, Hasan A (2012) Effect of dust accumulation on performance of photovoltaic solar modules in Sahara environment. J Basic Appl Sci Res 2(11):11030–11036
18. Menoufi K, Farghal HF, Farghali AA, Khedr MH (2017) Dust accumulation on photovoltaic panels: a case study at the East Bank of the Nile (Beni-Suef, Egypt). Energy Procedia 128:24–31
19. Shen L, Li Z, Ma T (2020) Analysis of the power loss and quantification of the energy distribution in PV module. Appl Energy 260:114333
20. Hanifi H, Pfau C, Turek M, Schneider J (2018) A practical optical and electrical model to estimate the power losses and quantification of different heat sources in silicon based PV modules. Renew Energy 127:602–612
21. Xu Z, Qu H, Li X, Zhao Y, Li Y and Han Z (2020) Theoretical model of optical transmission and reflection characteristics of dusty PV modules. Solar Energy Mater Solar Cells 213:110554
22. Gholami A, Ameri M, Zandi M, Ghoachani RG (2022) Electrical, thermal and optical modeling of photovoltaic systems: step-by-step guide and comparative review study. Sustain Energy Technol Assess 49:101711
23. Lu ZH, Yao Q (2007) Energy analysis of silicon solar cell modules based on an optical model for arbitrary layers. Sol Energy 81(5):636–647
24. Gholami A, Ameri M, Zandi M, Ghoachani RG, Kazem HA (2022) Predicting solar photovoltaic electrical output under variable environmental conditions: modified semi-empirical correlations for dust. Energy Sustain Dev 71:389–405
25. Shamim A, Noman M, Zubair M, Khan AD, Saher S (2018) A facile approach to determine the unknown refractive index (n) and extinction coefficient (k) of novel encapsulant materials used in back contact PV modules. Appl Phys A 124(8):1–6
26. Mishra SK and Goel V (2022) Modelling complex refractive indices of sub-micron pure and polluted dust based on compositional sensitive analysis. MAPAN-Journal of Metrology Society of India 37:1–11

27. Levin EJT, McMeeking GR, Carrico CM, Mack LE, Kreidenweis SM, Wold CE, Moosmüller H, Arnott WP, Hao WM, Collett Jr JL and Malm WC (2010) Biomass burning smoke aerosol properties measured during Fire Laboratory at Missoula Experiments (FLAME). J Geophys Res 115:D18210
28. Hemza A, Abdeslam H, Rachid C, Aoun N (2019) Simplified methods for evaluating the degradation of photovoltaic module and modeling considering partial shading. Measurement 138:217–224
29. Kamal R, Abdel-Salam M, Nayel M Estimation of photovoltaic module parameters based on datasheet: a review and a proposed method, submitted for publication in journal of engineering and applied science, Cairo, Egypt in 2022
30. ChinVJ SZ, Ishaque K (2015) Cell modelling and model parameters estimation techniques for photovoltaic simulator application: a review. Appl Energy 154:500–519
31. Sweelem EA, El Shenawy ET, Nafeh AA (2015) Effect of different dust accumulation on the performance of PV module in Egypt. Int J Adv Inform Sci Technol 44(44):1–10
32. Al-Ahmed A, Al-Sulaiman FA, Khan F (eds) (2022) The effects of dust and heat on photovoltaic modules: impacts and solutions. Springer International Publishing: Cham, Switzerland
33. Dubovik O, Holben B, Eck TF, Smirnov A, Kaufman YJ, King MD, Tanré D, Slutsker I (2002) Variability of absorption and optical properties of key aerosol types observed in worldwide locations. J Atmos Sci 59(3):590–608
34. Wagner R, Ajtai T, Kandler K, Lieke K, Linke C, Müller T, Schnaiter M, Vragel M (2012) Complex refractive indices of Saharan dust samples at visible and near UV wavelengths: a laboratory study. Atmos Chem Phys 12(5):2491–2512
35. Müller T, Schladitz A, Massling A, Kaaden N, Kandler K, Wiedensohler A (2009) Spectral absorption coefficients and imaginary parts of refractive indices of Saharan dust during SAMUM-1. Tellus B 61(1):79–95
36. Stapiński T, Marszałek K, Lipiński M, Panek P and Szczepanik W (2012) Investigations of solar panels with anhanced transmission glass. Microelectron Mater Technol 231:285–296
37. Rubin M (1985) Optical properties of soda lime silica glasses. Solar Energy Materials 12(4):275–288
38. Guan Y, Zhang H, Xiao B, Zhou Z, Yan X (2017) In-situ investigation of the effect of dust deposition on the performance of polycrystalline silicon photovoltaic modules. Renew Energy 101:1273–1284

Publisher's Note